

Article

Guidance-Based Path Following of an Underactuated Ship Based on Event-Triggered Sliding Mode Control

Yuxi Zhang and Yong Liu * 

College of Navigation, Dalian Maritime University, Dalian 116026, China

* Correspondence: liu_yong@dlnu.edu.cn

Abstract: In this paper, the path following of an underactuated ship as a fundamental application for autonomous sailing in seaways is studied. First, the guidance system based on the line of sight (LOS) method is established to handle underactuated dynamics of ship motion. Then, path following control is converted to heading control with fewer dimensions. Second, the extended state observer (ESO) is used to observe unknown dynamics of ship motion. Third, the sliding mode control method is highly robust to external disturbance and is employed to design the controller. Fourth, the event-triggered mechanism (ETM) is included to reduce the trigger time. All the closed-loop signals are shown to be bounded by the Lyapunov theory. Simulations are carried out to verify the effectiveness of the proposed method.

Keywords: path following; line of sight; sliding mode; event-triggered



Citation: Zhang, Y.; Liu, Y. Guidance-Based Path Following of an Underactuated Ship Based on Event-Triggered Sliding Mode Control. *J. Mar. Sci. Eng.* **2022**, *10*, 1780. <https://doi.org/10.3390/jmse10111780>

Academic Editors: Mai The Vu and Hyeung-Sik Choi

Received: 17 October 2022

Accepted: 15 November 2022

Published: 18 November 2022

Publisher's Note: MDPI stays neutral with regard to jurisdictional claims in published maps and institutional affiliations.



Copyright: © 2022 by the authors. Licensee MDPI, Basel, Switzerland. This article is an open access article distributed under the terms and conditions of the Creative Commons Attribution (CC BY) license (<https://creativecommons.org/licenses/by/4.0/>).

1. Introduction

According to the actuator configuration, the ship can be generally categorized as the fully actuated ship and underactuated ship. Promising results were presented for controlling the fully actuated ship in previous years [1–5]. Nevertheless, the underactuated ship is so far the most common configuration in reality [6]. Path following of the underactuated ship is the key technique for autonomous sailing, which is a fundamental and representative application at sea. The underactuated ship indicates that the freedom degrees of the control inputs are less than the control outputs, i.e., the sway direction of the underactuated ship is not directly actuated, leading to the theoretical challenge [6–8]. In this paper, path following control of the underactuated ship is studied due to its theoretical challenges and wide applications.

Path following control of the underactuated ship requires it to follow a prescribed path as accurately as possible with limited control actuators [9–11]. Generally, the previous results of the underactuated ship can be classified into two mainstreams, i.e., nonlinear control theory and guidance-based control theory. Taking advantage of the ship model, multiple previous results are obtained based on nonlinear control theory [12,13]; however, these results are either too complex or with restrictive assumption, e.g., persistent excitation (PE) condition. That is, the reference signal can be nonzero, i.e., the straight-line following which is the most common practice at sea is excluded. Guidance-based control otherwise is more prevalent nowadays due to its straightforward and practical characteristics [14,15]. Therefore, the guidance-based path following of the underactuated ship is studied herein.

The ship motion control consists of a guidance system, navigation system, and control system (GNC). The guidance system determines the reference or desired states, e.g., the desired route; the navigation system measures the current motion state of the ship, e.g., current position and speed; and the control system calculates the appropriate control maneuvers so that the ship tracks the reference state accurately as [14]. The literature [16] illustrates the design idea of guidance-based path following; then, a novel guidance law is also proposed. The line of sight (LOS) is employed into the control of the underactuated

ship [17]; subsequently, it attracted a great deal of attention from the ship motion control community [18–24]. A nonlinear adaptive strategy is presented for path following of the underactuated ship based on the LOS method with sideslip angle estimation [18]. The guidance principle for a sailboat based on LOS is developed, and the path following controller is designed with echo state networks (ESNs) to estimate the uncertainties [19]. The LOS guidance law is incorporated into the model predictive control (MPC), and then path following controller is designed [20]. The path-tangential reference frame is developed first; the path following controller is subsequently designed based on the dynamic surface control and iterative neural network [21]. By introducing the extended state observer (ESO) to identify the sideslip angle, the ESO-based LOS guidance law is presented for the path following controller [22]. The path following controller is designed based on the backstepping method with LOS guidance, where the neural network is used to estimate uncertainty of the model [23]. The neural path-following controller is designed for the underactuated ship based on the sliding mode and LOS method [24]. Ship sailing at sea would be inevitably influenced by the external disturbances. The sliding mode method is known as its robustness against external disturbances. Motivated by reference [24], the path following of the underactuated ship based on the sliding mode method is studied herein.

In reference [24], the control task is executed periodically with time-triggered strategy at any instant; in addition to the time-triggered strategy, the event-triggered strategy stirred extensive research interests in the control field due to its outstanding performance in efficiency [25–30]. The embedded microprocessors, which are normally used for information collecting and processing, are responsible for executing the control tasks. Because the computational resource is limited with embedded microprocessors at sea, it is interesting to develop the efficient path-following controller for the ship with event-triggered strategy. Thus, the event-triggered strategy for the nonlinear system [26] is employed herein, and it is then incorporated into the sliding mode control mechanism for designing the path-following controller of the underactuated ship herein. Furthermore, the active disturbance rejection control (ADRC) [31–33] is widely adopted for its simplicity and robustness against the unknown dynamics and external disturbances. It can estimate the unmodelled dynamics and external disturbance by means of the extended state observer (ESO).

It is proposed by [34] that a switched dynamical framework be used to model the interchanging phases and to formulate a comprehensive position control solution for heavy-lift vessels. Stability and robustness against modeling imperfections and environmental disturbances are analytically assessed. A new dynamic positioning (DP) method by an observer and a controller was composed by [35], and it is proposed to address system uncertainties, with stability guarantees in the presence of uncertainties. In [36], an observer-based robust controller is designed that can tackle model uncertainty in hydrodynamic damping and mooring forces, environmental disturbances can filter out the high-frequency vessel movement. An adaptive switched control framework that handles the uncertainty and switched dynamics without imposing structural constraints is proposed by [37]. Thus, the ESO [31–33] is included to estimate and compensate unknown model uncertainties in this paper. The main research contents are as follows.

1. The parameterized LOS guidance law is employed to lower dimensions of control outputs; then, the LOS guidance law is incorporated with the sliding mode method, where path following of the underactuated ship can be achieved through the heading control.
2. The event-triggered strategy can effectively reduce the trigger times. Once the trigger conditions meet the requirements, the control action will be activated immediately, leading to a practical and efficient guidance-based sliding mode controller for the underactuated ship's path following.
3. Unknown dynamics of ship motion is augmented as an extra state, and the extended state observer is included to handle it herein. Finally, an event-triggered-based sliding mode controller with ESO is presented for the path following of the underactuated ship herein.

2. Preliminaries and Problem Formulation

2.1. Kinematics

The ship motion can be generally categorized as kinematics and kinetics [14]. The kinematics of 3-degree of freedom (3-DoF) are as follows,

$$\begin{aligned} \dot{x} &= u \cos \psi - v \sin \psi \\ \dot{y} &= u \sin \psi + v \cos \psi \\ \dot{\psi} &= r \end{aligned} \tag{1}$$

where x denotes longitudinal displacement, y denotes lateral displacement, and ψ denotes yaw angle; u denotes surge velocity, v denotes sway velocity, and r denotes yaw rate [14].

The parameterized reference path can be described by $x_d(\omega)$ and $y_d(\omega)$, and the path-tangential reference frame is rotated as the angle [16,18,21],

$$\chi_d(\omega) = \arctan \frac{y'_d(\omega)}{x'_d(\omega)} \tag{2}$$

where $y'_d(\omega) = \partial y_d / \partial \omega$ and $x'_d(\omega) = \partial x_d / \partial \omega$.

The reference system can be written as

$$\begin{bmatrix} \dot{x}_d(\omega) \\ \dot{y}_d(\omega) \end{bmatrix} = \begin{bmatrix} \cos \chi_d & -\sin \chi_d \\ \sin \chi_d & \cos \chi_d \end{bmatrix} v_d \tag{3}$$

where $v_d = [U_p, 0]^T$ represents the ideal particle velocity [16].

From Equations (1)–(3), the following error system can be established:

$$\begin{bmatrix} \dot{x}_e \\ \dot{y}_e \end{bmatrix} = \begin{bmatrix} \cos \chi_d & -\sin \chi_d \\ \sin \chi_d & \cos \chi_d \end{bmatrix}^T \begin{bmatrix} \dot{x} - \dot{x}_d(\omega) \\ \dot{y} - \dot{y}_d(\omega) \end{bmatrix} \tag{4}$$

where x_e denotes along-track error and y_e denotes cross-track error [16].

Differentiate Equation (4), it has

$$\begin{aligned} \dot{x}_e &= u \cos(\psi - \chi_d) - v \sin(\psi - \chi_d) \\ &\quad - \dot{x}_d \cos \chi_d - \dot{y}_d \sin \chi_d + \dot{\chi}_d y_e \\ \dot{y}_e &= u \sin(\psi - \chi_d) + v \cos(\psi - \chi_d) \\ &\quad + \dot{x}_d \sin \chi_d - \dot{y}_d \cos \chi_d - \dot{\chi}_d x_e \end{aligned} \tag{5}$$

By substituting Equation (3) into Equation (5), it can be obtained

$$\begin{aligned} \dot{x}_e &= U \cos(\psi - \chi_d + \beta) + \dot{\chi}_d y_e - U_p \\ \dot{y}_e &= U \sin(\psi - \chi_d + \beta) - \dot{\chi}_d x_e \end{aligned} \tag{6}$$

where $U = \sqrt{u^2 + v^2}$ and $\beta = \arctan(v/u)$ [21]. Obviously, the geometric task is to drive x_e and y_e to zero. U_p can be viewed as a virtual input to be designed for Equation (6) [16,18,21].

Design the guidance law as

$$U_p = U \frac{\Delta}{\sqrt{\Delta^2 + y_e^2}} + l_1 x_e \tag{7}$$

$$\psi_d = \chi_d + \arctan\left(\frac{-y_e}{\Delta}\right) - \beta \tag{8}$$

where Δ denotes look-ahead distance and l_1 denotes a positive tunable parameter. ψ_d denotes the desired heading angle.

Define the following Lyapunov function,

$$V_1 = \frac{1}{2}x_e^2 + \frac{1}{2}y_e^2 \geq 0. \tag{9}$$

Differentiate Equation (9) and substitute Equations (6)–(8), it has

$$\begin{aligned} \dot{V}_1 &= x_e \dot{x}_e + y_e \dot{y}_e \\ &= x_e(-l_1 x_e + \dot{\chi}_d y_e) + y_e(-U \frac{y_e}{\sqrt{y_e^2 + \Delta^2}} - \dot{\chi}_d x_e) \\ &= -l_1 x_e^2 - l_2 y_e^2 \leq 0 \end{aligned} \tag{10}$$

where $l_2 = \frac{U}{\sqrt{y_e^2 + \Delta^2}} \geq 0$.

Above all, it can be concluded from Equations (9) and (10) that the system (6) with guidance law (7) and (8) is stable.

2.2. Kinetics

In this section, the kinetics of the simulation model are introduced, which is widely used in the references [21,38].

$$\begin{aligned} \dot{u} &= \frac{m_{22}}{m_{11}}vr - \frac{d_u}{m_{11}}u - \sum_{i=2}^3 \frac{d_{ui}}{m_{11}}|u|^{i-1}u + \frac{1}{m_{11}}\tau_u + \frac{1}{m_{11}}\tau_{wu} \\ \dot{v} &= -\frac{m_{11}}{m_{22}}ur - \frac{d_v}{m_{22}}v - \sum_{i=2}^3 \frac{d_{vi}}{m_{22}}|v|^{i-1}v + \frac{1}{m_{22}}\tau_{wv} \\ \dot{r} &= \frac{m_{11}-m_{22}}{m_{33}}uv - \frac{d_r}{m_{33}}r - \sum_{i=2}^3 \frac{d_{ri}}{m_{33}}|r|^{i-1}r + \frac{1}{m_{33}}\tau_r + \frac{1}{m_{33}}\tau_{wr} \end{aligned} \tag{11}$$

where u denotes surge velocity, v denotes sway velocity, and r denotes yaw rate. $m_{jj}(j = 1, 2, 3)$ denotes the ship inertia including added mass. $d_u, d_v, d_r, d_{ui}, d_{vi}$ and d_{ri} denote hydrodynamic damping. τ_{wu}, τ_{wv} , and τ_{wr} denote external disturbances. τ_u and τ_r denote surge force and yaw moment [21,38].

2.3. Problem Formulation

First, a guidance law based on the parameterized LOS method is designed [16,18,21]; then, the path following problem is achieved through heading control. Second, the sliding mode control method [39] is applied to design of control law. Third, a guidance-based sliding mode controller, which includes an event-triggering condition [25–30], is designed for solving the path following problem of the underactuated ship. Fourth, the extended state observer (ESO) is included to estimate unknown dynamics and disturbances [31–33], and the technical framework is given in Figure 1.

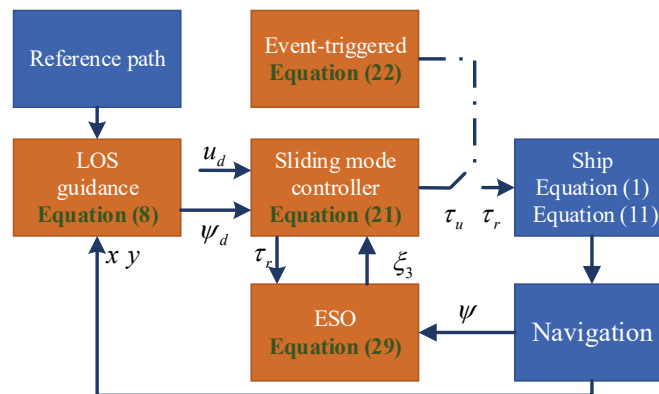


Figure 1. Technical framework for event-triggered-based sliding mode controller.

3. Controller Design

The controller design procedure includes the sliding mode controller, extended state observer, and event-triggered principle. First, the sliding mode control method is employed to design the controller for path following of the underactuated ship. Second, the event-triggering condition is designed and incorporated into the sliding mode controller; to this end, the event-triggered sliding mode controller is obtained. Third, the unknown dynamic of ship motion and the external disturbance are assumed to be a differentiated function f , which is estimated by the extended state observer.

3.1. Sliding Mode Design

Define $x_1 = \psi$ and $x_2 = r$; the control design model can be formulated as

$$\begin{aligned} \dot{x}_1 &= x_2 \\ \dot{x}_2 &= f + b\tau_r \end{aligned} \tag{12}$$

where $f = \frac{m_{11}-m_{22}}{m_{33}}uv - \frac{d_r}{m_{33}}r - \sum_{i=2}^3 \frac{d_{ri}}{m_{33}}|r|^{i-1}r + \frac{1}{m_{33}}\tau_{wr}$ and $b = \frac{1}{m_{33}}$.

Define the heading error as

$$z_1 = x_1 - \psi_d. \tag{13}$$

The first sliding mode surface can be designed as

$$s_1 = \dot{z}_1 + c_1z_1. \tag{14}$$

Differentiate Equation (14), it has

$$\begin{aligned} \dot{s}_1 &= \ddot{z}_1 + c_1\dot{z}_1 \\ &= f + b\tau_r - \ddot{\psi}_d + c_1\dot{z}_1 \end{aligned} \tag{15}$$

The equivalent part of the sliding mode controller can be design as

$$\tau_{req} = \frac{1}{b} \left(-c_1\dot{z}_1 - f + \ddot{\psi}_d \right) \tag{16}$$

where c_1 is a positive controller parameter.

Define the following Lyapunov function,

$$V_1 = \frac{1}{2}s_1^2 \geq 0. \tag{17}$$

Differentiate Equation (17), it has

$$\begin{aligned} \dot{V}_1 &= s_1\dot{s}_1 \\ &= s_1 \left[f + b(\tau_{req} + \tau_{rsw}) - \ddot{\psi}_d + c_1\dot{z}_1 \right] \end{aligned} \tag{18}$$

Substitute Equation (16) into the Equation (18), it has

$$\dot{V}_1 = s_1(b\tau_{rsw}). \tag{19}$$

The switch part of the sliding mode controller is

$$\tau_{rsw} = \frac{1}{b} [-k_1s_1 - \eta_1\text{sign}(s_1)]. \tag{20}$$

where k_1 and η_1 are positive controller parameters.

3.2. Event-Triggering Design

The event-triggered sliding mode controller is designed as

$$\tau_{rw} = \frac{1}{b} \left[-k_1 s_1 - \eta_1 \text{sign}(s_1) - c_1 \dot{z}_1 - f + \ddot{\psi}_d \right] + \left[-\bar{m} \tanh\left(\frac{s_1 \bar{m}}{\varepsilon}\right) \right] \tag{21}$$

and the triggering event is designed as

$$\begin{aligned} \tau_r(t) &= \tau_{rw}(t_k), \forall t \in [t_k, t_{k+1}) \\ t_{k+1} &= \inf\{t \in \mathbb{R} \mid |e(t)| \geq m\}, t_1 = 0 \end{aligned} \tag{22}$$

where $e(t) = \tau_{rw}(t) - \tau_r(t)$ denotes a measurement error. ε , m , and $\bar{m} > m$ are positive event-triggering parameters. t_k denotes the update time of the event-triggered-based controller. Note that in $t \in [t_k, t_{k+1})$ the controller is constant [26].

Now, the stability of the event-triggered sliding mode controller is analyzed. By employing a new parameter $\lambda(t)$, such that

$$\tau_{rw} = \tau_r + \lambda(t)m \tag{23}$$

where $\lambda(t_k) = 0, |\lambda(t)| \leq 1, \forall t \in [t_k, t_{k+1})$, and $\lambda(t_{k+1}) = \pm 1$.

Substitute Equations (21) and (23) into Equation (18), it can be obtained

$$\begin{aligned} \dot{V}_1 &= s_1 \dot{s}_1 \\ &= s_1 \left[-k_1 s_1 - \eta_1 \text{sign}(s_1) + b \left(-\bar{m} \tanh\left(\frac{s_1 \bar{m}}{\varepsilon}\right) - \lambda(t)m \right) \right] \\ &= -k_1 s_1^2 - \eta_1 |s_1| + b \left(-s_1 \bar{m} \tanh\left(\frac{s_1 \bar{m}}{\varepsilon}\right) - \lambda(t)m s_1 \right). \end{aligned} \tag{24}$$

Define $\rho = s_1 \bar{m}$, Equation (24) can be rewritten as

$$\begin{aligned} \dot{V}_1 &= s_1 \dot{s}_1 \\ &\leq -k_1 s_1^2 - \eta_1 |s_1| + b(|\rho| - \rho \tanh\left(\frac{\rho}{\varepsilon}\right)). \end{aligned} \tag{25}$$

Note it has the following relation [26,40]

$$0 \leq |\rho| - \rho \tanh\left(\frac{\rho}{\varepsilon}\right) \leq 0.2785\varepsilon. \tag{26}$$

Thus,

$$\dot{V}_1 \leq -k_1 s_1^2 - \eta_1 |s_1| + \gamma_0. \tag{27}$$

Note that b and ε are both positive parameters, so $\gamma_0 = 0.2785b\varepsilon$ is bounded. From Equations (17)–(27), all signals in the closed-loop system together with the event-triggered sliding mode controller (22) are bounded based on the Lyapunov theorem. The system is globally stable in the sense that the tracking error will exponentially converge towards a set, which is adjustable by choosing suitable parameters.

3.3. Extended State Observer

By employing a new state $x_3 = f$, the system (12) can be extended into the following system

$$\begin{aligned} \dot{x}_1 &= x_2 \\ \dot{x}_2 &= x_3 + b\tau_r \\ \dot{x}_3 &= \dot{f} \\ y &= x_1 \end{aligned} \tag{28}$$

It is assumed that f can be differentiated since the dynamic is time-varying [31,32]. Then, we can design the ESO for (28),

$$\begin{aligned} \alpha_1 &= \xi_1 - y \\ \dot{\xi}_1 &= \xi_2 - \beta_1 \alpha_1 \\ \dot{\xi}_2 &= \xi_3 - \beta_2 \alpha_1 + b\tau_r \\ \dot{\xi}_3 &= -\beta_3 \alpha_1 \end{aligned} \tag{29}$$

where ε_1 denotes the approximation error. ξ_1 and ξ_2 approximate x_1 and x_2 , respectively; ξ_3 approximates f . β_1, β_2 , and β_3 are observer gain, and it can be tuned by

$$\beta_1 = 3\omega_0, \beta_2 = 3\omega_0^2, \beta_3 = \omega_0^3 \tag{30}$$

where ω_0 is the observer bandwidth [31,32]. The ESO can be convergent by properly selecting the observer gain $s^3 + \beta_1s^2 + \beta_2s + \beta_3 = (s + \omega)^3$ as Hurwitz.

Above all, the presented event-triggered sliding mode controller with the ESO of yaw moment can be designed as follows

$$\tau_r = \frac{1}{b} \left[-k_1s_1 - \eta_1 \text{sign}(s_1) - c_1\dot{z}_1 - \xi_3 + \ddot{\psi}_d \right] + \left[-\bar{m} \tanh\left(\frac{s_1 \bar{m}}{\varepsilon}\right) \right]. \tag{31}$$

4. Simulation Results

Simulations are conducted to verify the presented event-triggered-based sliding mode controller for path following of the underactuated ship. Controller for surge force is used as follows:

$$\tau_u = m_{11} \left[-c_2z_2 + \dot{u}_d - f_u - \eta_2 \text{sign}(z_2) \right] \tag{32}$$

where $f_u = \frac{m_{22}}{m_{11}}vr - \frac{d_u}{m_{11}}u - \sum_{i=2}^3 \frac{d_{ui}}{m_{11}}|u|^{i-1}u$, $z_2 = u - u_d$, and u_d is the desired velocity.

c_2 and η_2 are both positive parameters. The model parameters are $m_{11} = 120 \times 10^3$, $m_{22} = 177.9 \times 10^3$, $m_{33} = 636 \times 10^5$, $d_u = 215 \times 10^2$, $d_v = 147 \times 10^3$, $d_r = 802 \times 10^4$, $d_{u2} = 0.2d_u$, $d_{u3} = 0.1d_u$, $d_{v2} = 0.2d_v$, $d_{v3} = 0.1d_v$, $d_{r2} = 0.2d_r$, and $d_{r3} = 0.1d_r$ [21]. The sampling instant is $t_s = 0.01$ and desired velocity is $u_d = 0.5$ [21]. The controller parameters $c_1 = 10, k_1 = 10, c_2 = 0.5, \eta_1 = 0.001, \eta_2 = 0.001, l_1 = 0.1, \Delta = 3$. The external disturbance is set as $\tau_{wu} = \tau_{wv} = \tau_{wr} = 10^3[1 + \sin(0.1t)]$.

4.1. Straight Path Following

The performance of the event-triggered-based sliding mode controller of straight path following is investigated. The simulation results are given in Figures 2–4. In Figure 2, the red line is the reference signal; then, the guidance system is established based the LOS method, and the guidance path is given in the green dot. The blue dot is the ship route of path following. Figure 2 shows that the ship can follow the desired path as closely as possible.

Figure 3 depicts yaw moment and surge force. Figure 4 depicts the estimation with ESO. It can be seen that the states and unknown dynamics can be estimated by the ESO, and straight path following is achieved by the proposed event-triggered-based sliding mode controller with ESO.

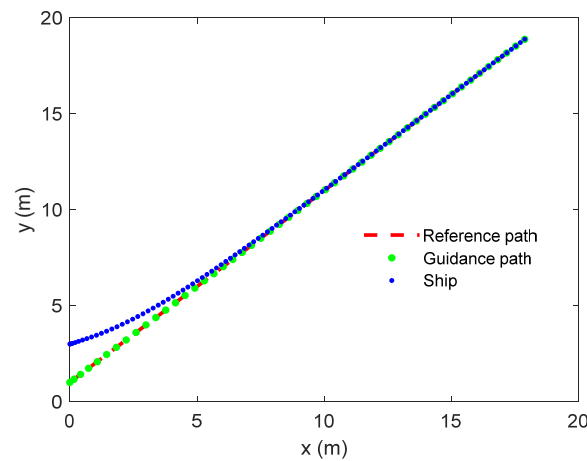


Figure 2. The performance of straight path following.

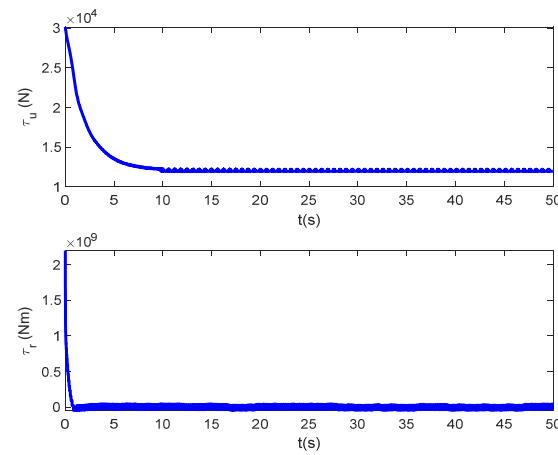


Figure 3. The yaw moment and surge force.

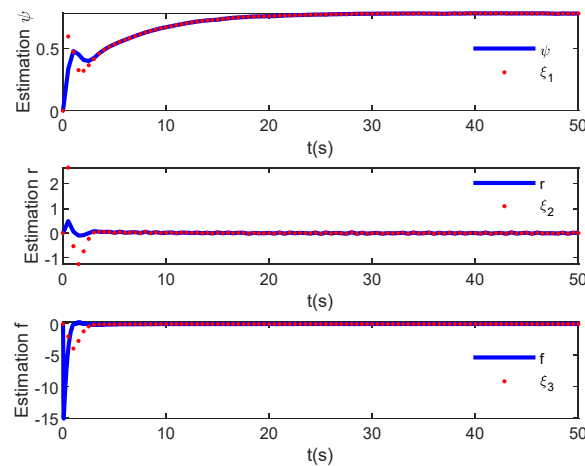


Figure 4. The estimation with ESO.

4.2. Curved Path Following

The performance of the event-triggered-based sliding mode controller for curved path following is investigated. In Figure 5, the red line is the reference signal; the guidance system is established based LOS method, and the guidance path is given by the green dot. The blue dot is the ship route of path following. Figure 5 shows that the ship can follow the desired path as closely as possible. Figure 6 shows the surge force and yaw

moment, respectively. Figure 7 shows the estimation with ESO. It can be seen that the states and dynamics can be estimated by the presented ESO, and the curved path following of the underactuated ship can be achieved by the presented even-triggered sliding mode controller with ESO.

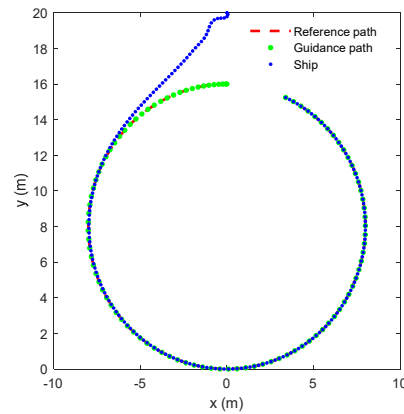


Figure 5. The performance of curved path following.

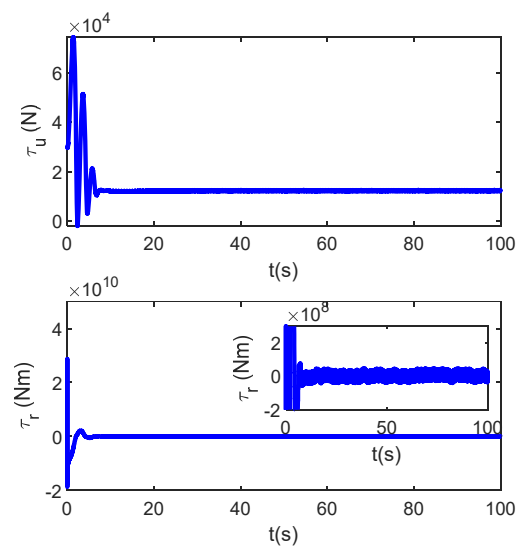


Figure 6. The yaw moment and surge force in curved-line path following.

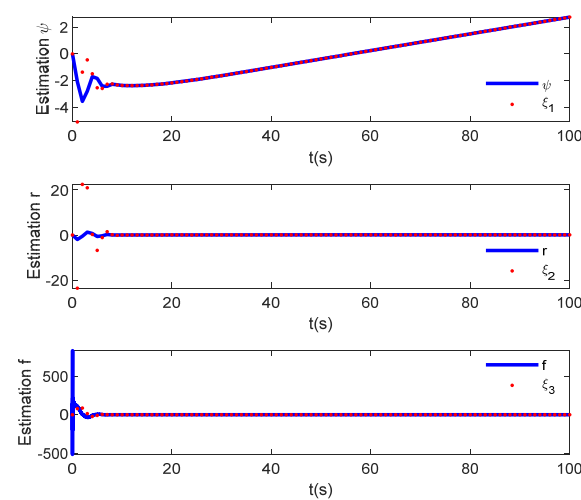


Figure 7. The estimation with ESO in curved-line path following.

4.3. Comparative Study

To illustrate the effectiveness of the proposed event-triggered-based sliding mode controller, comparative study between sliding mode controller [24] and event-triggered-based sliding mode controller is conducted. The results are shown in Table 1.

Table 1. The comparative results on triggering times.

Triggering Times	Sliding Mode Controller	Even-Triggered Sliding Mode Controller
Straight path following	5000	491
Curved path following	10,000	1106

Because $t_s = 0.01$ and the simulation time in straight path following is 50 s, the triggering times for conventional sliding mode controller is therefore 5000 times; the simulation time in curved-line path following is 100 s, the triggering times for the conventional sliding mode controller are therefore 10,000 times. The triggering times with the proposed event-triggered-based sliding mode controller is 491 times in straight path following and 1106 times in curved path following. It shows that the triggering time is reduced in both straight path and curved path following.

Above all, it shows that both straight path and curved path following can be achieved by the proposed event-triggered-based sliding mode controller with efficiency.

5. Conclusions

In the paper, a novel event-triggered-based sliding mode controller with ESO was designed for solving the path following control problem of the underactuated ship. A guidance system based on the LOS method was established to transform the control of path following into heading control. Second, sliding mode control is employed to design the heading controller. Third, the ESO was used to estimate the unknown dynamics and external disturbance. Fourth, the event-triggered principle was employed to reduce triggering times. Control system stability is guaranteed by the Lyapunov theorem. The simulation results verify the effectiveness and efficiency of the event-triggered sliding mode controller.

Author Contributions: Conceptualization, Y.Z.; methodology, Y.L.; software, Y.Z.; validation, Y.L.; formal analysis, Y.Z.; investigation, Y.L.; resources, Y.Z.; data curation, Y.L.; writing—original draft preparation, Y.Z.; writing—review and editing, Y.L.; visualization, Y.Z.; supervision, Y.L.; project administration, Y.Z.; funding acquisition, Y.L. All authors have read and agreed to the published version of the manuscript.

Funding: This work was supported by “Education Science “TEN-THREE-FIVE” Plan Project of Liaoning Province, China, 2020” (Number: JG20DB056).

Institutional Review Board Statement: Not applicable.

Informed Consent Statement: Not applicable.

Data Availability Statement: Not applicable.

Conflicts of Interest: The authors declare no conflict of interest.

References

- Zhu, G.; Du, J. Global Robust Adaptive Trajectory Tracking Control for Surface Ships Under Input Saturation. *IEEE J. Ocean. Eng.* **2018**, *45*, 442–450. [[CrossRef](#)]
- Du, J.; Yang, Y.; Wang, D.; Guo, C. A robust adaptive neural networks controller for maritime dynamic positioning system. *Neurocomputing* **2013**, *110*, 128–136. [[CrossRef](#)]
- Wang, Y.; Wang, H.; Li, M.; Wang, D.; Fu, M. Adaptive fuzzy controller design for dynamic positioning ship integrating prescribed performance. *Ocean Eng.* **2021**, *219*, 107956. [[CrossRef](#)]

4. Du, J.; Hu, X.; Liu, H.; Chen, C.L.P. Adaptive Robust Output Feedback Control for a Marine Dynamic Positioning System Based on a High-Gain Observer. *IEEE Trans. Neural Netw. Learn. Syst.* **2015**, *26*, 2775–2786. [[CrossRef](#)] [[PubMed](#)]
5. Wang, N.; Gao, Y.; Yang, C.; Zhang, X.F. Reinforcement learning-based finite-time tracking control for an unknown unmanned surface vehicle with input constraints. *Neurocomputing* **2022**, *484*, 26–37. [[CrossRef](#)]
6. Do, K. Global robust adaptive path-tracking control of underactuated ships under stochastic disturbances. *Ocean Eng.* **2016**, *111*, 267–278. [[CrossRef](#)]
7. Wang, N.; Su, S.-F.; Pan, X.; Yu, X.; Xie, G. Yaw-Guided Trajectory Tracking Control of an Asymmetric Underactuated Surface Vehicle. *IEEE Trans. Ind. Inform.* **2018**, *15*, 3502–3513. [[CrossRef](#)]
8. Wang, N.; Ahn, C.K. Hyperbolic-tangent LOS guidance-based finite-time path following of underactuated marine vehicles. *IEEE Trans. Ind. Electron.* **2020**, *67*, 8566–8575. [[CrossRef](#)]
9. Zhao, B.; Zhang, X.; Liang, C. A novel path-following control algorithm for surface vessels based on global course constraints and nonlinear feedback technology. *Appl. Ocean Res.* **2021**, *111*, 102635. [[CrossRef](#)]
10. Zhang, G.Q.; Zhang, C.L.; Yang, T.T.; Zhang, W.D. Disturbance observer-based composite neural learning path following control of underactuated ships subject to input saturation. *Ocean Eng.* **2020**, *216*, 108033. [[CrossRef](#)]
11. Liu, Z. Improved ELOS based path following control for underactuated surface vessels with roll constraints. *Ocean Eng.* **2022**, *245*, 110348. [[CrossRef](#)]
12. Lefeber, E.; Pettersen, K.; Nijmeijer, H. Tracking control of an underactuated ship. *IEEE Trans. Control Syst. Technol.* **2003**, *11*, 52–61. [[CrossRef](#)]
13. Do, K.; Jiang, Z.; Pan, J. Underactuated ship global tracking under relaxed conditions. *IEEE Trans. Autom. Control* **2002**, *47*, 1529–1536. [[CrossRef](#)]
14. Fossen, T.I. *Handbook of Marine Craft Hydrodynamics and Motion Control*; Wiley: London, UK, 2011.
15. Zhang, C.L.; Zhang, G.Q.; Zhang, X.K. DVSL guidance-based composite neural path following control for underactuated cable-laying vessels using event-triggered inputs. *Ocean Eng.* **2021**, *238*, 109713. [[CrossRef](#)]
16. Breivik, M.; Fossen, T.I. Principles of guidance-based path following in 2D and 3D. In Proceedings of the 44th IEEE Conference on Decision and Control, and the European Control Conference, Seville, Spain, 12–15 December 2005.
17. Fossen, T.I.; Breivik, M.; Skjetne, R. Line-of-sight path following of underactuated marine craft. In Proceedings of the IFAC Manoeuvring and Control of Marine Craft, Girona, Spain, 17–19 September 2003.
18. Fossen, T.I.; Pettersen, K.Y.; Galeazzi, R. Line-of-sight path following for Dubins paths with adaptive sideslip compensation of drift forces. *IEEE Trans. Control Syst. Technol.* **2015**, *23*, 820–827. [[CrossRef](#)]
19. Deng, Y.J.; Zhang, X.K.; Zhang, G.Q. Line-of-sight-based guidance and adaptive neural path-following control for sailboats. *IEEE J. Ocean. Eng.* **2020**, *45*, 1177–1188. [[CrossRef](#)]
20. Liu, C.; Wang, D.; Zhang, Y.; Meng, X. Model predictive control for path following and roll stabilization of marine vessels based on neurodynamic optimization. *Ocean Eng.* **2020**, *217*, 107524. [[CrossRef](#)]
21. Liu, L.; Wang, D.; Peng, Z. Path following of marine surface vehicles with dynamical uncertainty and time-varying ocean disturbances. *Neurocomputing* **2016**, *173*, 799–808. [[CrossRef](#)]
22. Liu, L.; Wang, D.; Peng, Z. ESO-Based Line-of-Sight Guidance Law for Path Following of Underactuated Marine Surface Vehicles With Exact Sideslip Compensation. *IEEE J. Ocean. Eng.* **2016**, *42*, 477–487. [[CrossRef](#)]
23. Liu, C.; Philip Chen, C.L.; Zou, Z.J.; Li, T.S. Adaptive NN-DSC control design for path following of underactuated surface vessels with input saturation. *Neurocomputing* **2017**, *267*, 466–474. [[CrossRef](#)]
24. Yu, Y.; Guo, C.; Yu, H. Finite-Time PLOS-Based Integral Sliding-Mode Adaptive Neural Path Following for Unmanned Surface Vessels with Unknown Dynamics and Disturbances. *IEEE Trans. Autom. Sci. Eng.* **2019**, *16*, 1500–1511. [[CrossRef](#)]
25. Tabuada, P. Event-Triggered Real-Time Scheduling of Stabilizing Control Tasks. *IEEE Trans. Autom. Control* **2007**, *52*, 1680–1685. [[CrossRef](#)]
26. Xing, L.; Wen, C.Y.; Liu, Z.T.; Su, H.Y.; Cai, J.P. Event-triggered adaptive control for a class of uncertain nonlinear systems. *IEEE Trans. Autom. Control* **2017**, *62*, 2071–2076. [[CrossRef](#)]
27. Wang, A.; Liu, L.; Qiu, J.; Feng, G. Event-Triggered Robust Adaptive Fuzzy Control for a Class of Nonlinear Systems. *IEEE Trans. Fuzzy Syst.* **2018**, *27*, 1648–1658. [[CrossRef](#)]
28. Wang, L.; Chen, C.L.P.; Li, H. Event-Triggered Adaptive Control of Saturated Nonlinear Systems With Time-Varying Partial State Constraints. *IEEE Trans. Cybern.* **2018**, *50*, 1485–1497. [[CrossRef](#)]
29. Huang, C.; Zhang, X.; Zhang, G. Decentralized event-triggered cooperative path-following control for multiple autonomous surface vessels under actuator failures. *Appl. Ocean Res.* **2021**, *113*, 102751. [[CrossRef](#)]
30. Li, J.; Zhang, G.; Zhang, X.; Zhang, W. Event-triggered robust adaptive control for path following of the URS in presence of the marine practice. *Ocean Eng.* **2021**, *242*, 110139. [[CrossRef](#)]
31. Gao, Z. Active disturbance rejection control: A paradigm shift in feedback control system design. In Proceedings of the 2006 American Control Conference, Minneapolis, MN, USA, 14–16 June 2006.
32. Yan, W.; Wang, L.F.; Zhang, J.Z.; Li, F. Path following control of autonomous ground vehicle based on nonsingular terminal sliding mode and active disturbance. *IEEE Trans. Veh. Technol.* **2019**, *68*, 6379–6390.
33. Zhang, G.; Zhang, C.; Zhang, X.; Deng, Y. ESO-based path following control for underactuated vehicles with the safety prediction obstacle avoidance mechanism. *Ocean Eng.* **2019**, *188*, 106259. [[CrossRef](#)]

34. Ye, J.; Roy, S.; Godjevac, M.; Baldi, S. A Switching Control Perspective on the Offshore Construction Scenario of Heavy-Lift Vessels. *IEEE Trans. Control Syst. Technol.* **2021**, *29*, 470–477. [[CrossRef](#)]
35. Ye, J.; Roy, S.; Godjevac, M. Robustifying Dynamic Positioning of Crane Vessels for Heavy Lifting Operation. *IEEE/CAA J. Autom. Sin.* **2021**, *8*, 753–765. [[CrossRef](#)]
36. Ye, J.; Roy, S.; Godjevac, M.; Baldi, S. Observer-based Robust Control for Dynamic Positioning of Large-Scale Heavy Lift Vessels. *IFAC-Pap. Line* **2019**, *52*, 138–143. [[CrossRef](#)]
37. Roy, S.; Baldi, S.; Ioannou, P.A. An Adaptive Control Framework for Underactuated Switched Euler–Lagrange Systems. *IEEE Trans. Autom. Control* **2022**, *67*, 4202–4209. [[CrossRef](#)]
38. Do, D.; Jiang, Z.; Pan, J. Robust adaptive path following of underactuated ships. *Automatica* **2004**, *40*, 929–944. [[CrossRef](#)]
39. Young, K.D.; Utkin, V.I.; Zguner, U.O. A control engineer’s guide to sliding mode control. *IEEE Trans. Control Syst. Technol.* **1999**, *7*, 328–342. [[CrossRef](#)]
40. Ren, B.; San, P.P.; Ge, S.S.; Lee, T.H. Adaptive dynamic surface control for a class of strict-feedback nonlinear systems with unknown backlash-like hysteresis. In Proceedings of the 2009 American Control Conference, St. Louis, MO, USA, 10–12 June 2009; pp. 4482–4487.